Dmytro SNIZHKO[1], Anatoliy KUKOBA[1]

Laboratory of Optochemotronics, Kharkiv National University of Radio Electronics (1), Ukraine

doi:10.15199/48.2019.08.24

Ultrafast Potentiostat as Compromise between Current Sensitivity vs. Response Time

Abstract. *Physical and technical problems of a potentiostat scheme are analyzed. Current sensitivity of the traditional potentiostat scheme is considered. The classical scheme of potentiostat was investigated to overcome the bounds of potentiostat perfection. The new scheme of ultrafast potentiostat is proposed, and its development principles are discussed. Improving potentiostat technical parameters such as response time, frequency bandwidth, stability, and potential range are clarified. Schematic simulation results and tests with a real electrochemical composition are shown.*

Streszczenie. *Analizowano techniczne I fizyczne problemy projektowania układu potencjostatu. Zaprojektowano nowy układ szybkiego potencjostatu biorąc pod uwagę czas odpowiedzi, pasmo częstotliwości i stabilność.* ***Ultraszybki potencjostat jako kompromis między czułością prądową I czasem odpowiedzi***

Keywords: Potentiostat, ultrafast voltammetry, microelectrodes, ohmic voltage drop compensation.
Słowa kluczowe: in the case of foreign Authors in this line the Editor inserts Polish translation of keywords.

Introduction

This work is considered to the problem of the response time of instrumentation with saving of sensitivity in electrochemical measurements. As authors [1] claims "The ability to measurement nA to pA currents at nanosecond timescales remains a challenge." It is a traditional problem of engineers that is a decrease of measurement current range and response time, i.e. an increase current sensitivity of a potentiostat and an enlarge bandwidth for an analytical signal is. To save the current sensitivity of potentiostat for higher signal time resolution the reduction of a charge registration limit is asked that is limited by a noise level of electronic components. As an example of this problem, the modern femtoampere amplifier LMP7721 by Texas Instrument which has typical input bias current at 3 fA and input-referred current noise at 0.01 pA/Hz$^{-1/2}$. For a current detection limit at 10 fA the measurement bandwidth reaches (current detection level/input current noise)^2 =1 Hz, i.e. time resolution for measurements is 1 s, amount of electrons for detection by the amplifier is greater than 6 000 electrons. So the physical limit of modern electronics is greater than a single electron detection level for a real potentiostat circuit. Electronic elements as wires, semiconductors chips, resistors, and others have electronic noises which specify a detection level in an electrical circuit, and its reduction to absolute zero level is practically impossible.

On the other hand, the utilization of novel construction technics and measurement methods can overcome limiting factors. In this paper, we try to analyze the construction of a tradition potentiostat to decrease the response time to nanosecond resolution and to determine sensitivity which we can obtain with commercial operational amplifiers.

Investigations of possibilities to construct an ultrafast potentiostat as well as its utilization were considered in different articles [2-20]. The theoretical basis of the electrochemistry in fast polarization modes has been studied by C. Amatore and co-workers [1, 21]. The reasonable investigations also present in [22-24].

In this paper, we attempt to generalize the experience of the ultrafast potentiostat construction as the concept of its building and to evaluate its features for the actual design.

In this work, we try to recognize a practical detection level for fast electrochemical measurements with commercially available electronics. The aim of this work is a search of a possibility to construct a potentiostat with a megavolt per second range sweep rate ability and with a minimum current detection limit. The analyses of the potentiostat scheme and a description of ultrafast potentiostat (UFP) principles were done. The constructed UFP modeling in the electronics engineering software and testing in an electrochemical experiment are described in the paper.

Commercial potentiostats have features for stable work with different cells and electrodes systems, as a rule, they have not short time resolution characteristics. In some of them is realized an ohmic voltage drop compensation with a short time break of a measurement circuit that also limits a circuit bandwidth. In other an ohmic voltage drop compensation is an interstage positive feedback loop between a control amplifier and a current-to-voltage converter. This also requires a bandwidth limitation features for a circuit. Bounded possibilities in ultrafast electrochemical technics restrain investigations in this direction. The rising interest in a field of single molecule analysis, nanomaterial applications in electrochemistry, films investigations and electrochemical catalytic reaction studies stimulates an activity directed to increase potentiostat capabilities.

Analysis of potentiostat constructing problem

The main purpose of a potentiostat is a control of a potential difference (or simply potential) at an interface between a working electrode and an electrochemical cell inner solution. Functionally a potentiostat circuit can be implemented by using a single operational amplifier [11], but it is limited due to the need to combine signals from sources, one of them (a reference electrode) has a high output impedance. So an additional stage of a voltage follower is required in the circuit. Additionally, an analytical potentiostat should have a possibility to measure a current flowed through an electrochemical cell. A corresponding stage should be in the potentiostat circuit. Thus, a potentiostat includes three stages: the control amplifier, the voltage follower, the current-to-voltage converter [25]. This concept is most usable in commercial potentiostats. Real schemes of commercial potentiostats are more complex, and they have different units for signal filtering and scaling. Sometimes they support four-electrode cell operation and ohmic voltage drop compensation. [25-26] Floating potentiostats have galvanic separated measurement circuit from the ground, but it does not effect on principles of its operation.

Ultrafast potentiostat construction

To construct an ultrafast potentiostat, a simple solution to take a classical scheme of a potentiostat and to use

modern electronics does not give a desired effect. A variety of phenomena occurs at high frequencies. In the absence of a frequency limit for a signal, the instability leads to a generation in a potentiostat circuit. An interstage phase shift for operational amplifiers is raised at a high frequency that demolishes the stability of a potentiostat operation.

In a construction of UFP we are proposing to utilize the following principles.

i) Do not use interstage feedback loops. Since the general gain for stages closed by one feedback loop can change by the magnitude and the sign when a summarize interstage phase shift will be sufficient at high frequencies, respectively, it will lead to a generation in a circuit and its instability.

ii) Minimize number of active components. Minimum of components is used for a realization of principal units (the control amplifier, the voltage follower and the current-to-voltage converter). It ensures a fast transmission of an electrical signal in a circuit.

iii) The ohmic voltage drop compensation is necessary to implement in the current-to-voltage converter stage. With an increase of scan rate (processing at high frequencies) a compensation of an ohmic voltage drop in a cell solution is important as this factor increases an influence with a rise of a working frequency. Since a current measurement is processed in the current-to-voltage converter unit, and implementation of interstage connections is forbidden according to the first principle, so the ohmic voltage drop compensation is needed to realize in the current measurement stage.

The potentiostat scheme satisfies above principles is shown in Fig. 1.

UFP operation is based on principles of the classical scheme. The measurement scheme of the equilibrium potential remains unchanged since it is a problem to offer an alternative scheme for a non-inverting voltage follower. Nevertheless, in a voltage follower, an operational amplifier will not cope with the quick formation of a response when increase a frequency of a cell excitation signal.

At a certain frequency, a phase shift value between the operational amplifier in follower and the control operational amplifier can be sufficient which leads to a generation and unstable operation of the whole potentiostat. To prevent this, after the voltage follower the RCR-filter is included. It prevents a high-frequency signal propagation to the amplifier in the control stage. Accordingly, a signal about the equilibrium potential from a reference electrode lay in a frequency range where a phase shift between operational amplifier stages of the potentiostat and of the follower is insignificant.

To transfer an excitation signal, the frequency bandwidth for a control stage should stay high. In a common case, the voltage follower signal is the feedback signal for the control stage. Since in our circuit the bandwidth frequency is limited, so we have to introduce an additional feedback loop what determines an operational mode for the control amplifier. To eliminate the potentiostat self-excitation, the local feedback loop of the control amplifier switches the gain to unity for signals with frequencies higher than the cut-off frequency of the filter. This loop is a serial RC-circuit its parameters are chosen so that the amplification is unity for the signal with frequencies above the cut-off frequency of RCR-filter after the follower stage.

Additionally, in the circuit the input buffer stage added for an excitation signal from a source connected by the 50Ω-impedance coaxial cable. This solution is necessary for a high-frequency signal transmission without distortion.

The low-frequency signal may be introduced into the circuit without passing through the buffer stage over R2 resistor.

We consider realizing the ohmic voltage drop compensation in the current-to-voltage converter stage so that the operational amplifier is used with positive and negative feedback loops in this stage. The compensation branch is resistive voltage divider that is added to the classical current-to-voltage converter circuit based on an operation amplifier [27]. So, one branch is the negative feedback and it determines a conversion factor, other is the positive feedback that compensates the voltage drop in a cell. This circuit can work stable until a depth of the negative feedback is greater than the positive feedback. The compensation resistance is equivalent to value R6×R8/R7. When R6 and R7 are the same, it is R8.

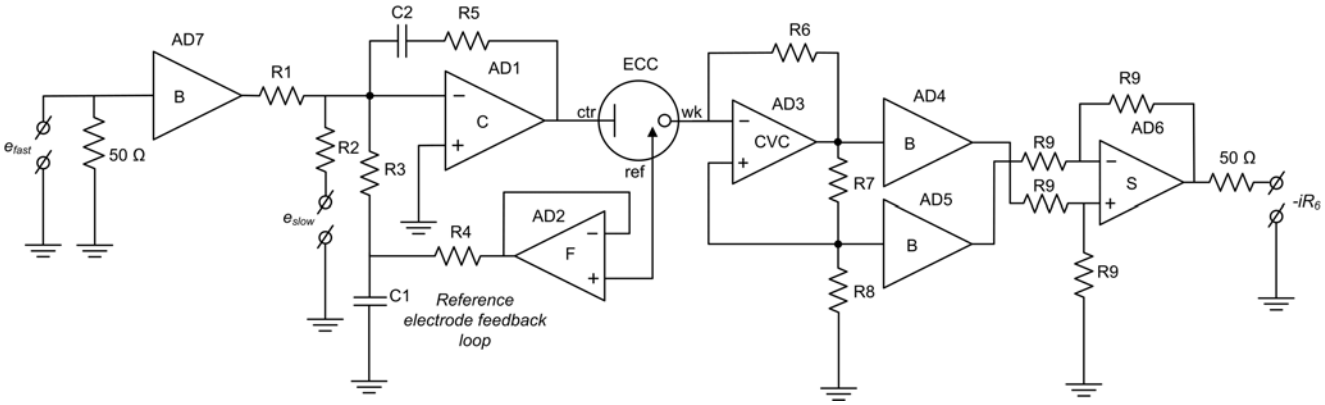

Fig.1. The ultrafast potentiostat scheme. B – buffer, C – control amplifier, F – follower, CVC – current-to-voltage converter, S – substractor, ECC – electrochemical cell, ctr – counter electrode, ref – reference electrode, wk – working electrode, e_{fast} – fast control signal for ECC, e_{slow} – slow control signal for ECC, $-iR_6$ – response signal.

Let's consider how it works. An output voltage signal of the current-to-voltage converter is proportional to a current through a cell in accordance with a resistor value in a negative feedback loop, R6. The resistive divider takes a signal that equal to a value of a potential drop on a solution ohmic resistance. This compensation signal is fed to the non-inverting input of the current-to-voltage converter amplifier, and the offset potential drives the inverting input of the amplifier accordingly to the operation amplifier processing. The working electrode connected to the inverting input is shifted on the magnitude of losses. Since this function is continuous, the compensation is possible in a whole working frequency range for the current-to-voltage converter frequency bandwidth. A side effect is that the output signal also gets some shift, and it is eliminated by the subtractor on the unit output. To prevent the subtractor

stage operation effects on the current-to-voltage converter operation, the converter output signal and the resistive voltage divider signal are buffered. The output signal of the subtractor is free from a compensation part and proportional to a current through a cell. Since an interstage link is absent here, it is not contrary to above-accepted principles for the ultrafast potentiostat construction. By the way, the signals are distributed over symmetrical branches. The accumulated time delay is fixed in the three amplifier stages in the current-to-voltage converter unit so it can be taken into account and be compensated in the experiment.

It's one principal question why UFP should work in a follower mode at frequencies greater than the bandwidth limit for the reference voltage follower. The engineering solution to this question was obtained by analysis of what a potentiostat circuit should do when the feedback bandwidth is not satisfied with the excitation signal bandwidth. Because an equilibrium potential as a signal of a reference electrode is a thermodynamic factor, it is not changing quickly in the whole volume of a cell, if electrolysis is accomplished by a short time pulse [7,8]. As the equilibrium potential determination does not ask a very quick measurement, so a response frequency for this signal is possible limiting in a circuit [3].

The application of a counter electrode with a bigger area than a working electrode guarantees that a total impedance of two electrode interfaces will only be determined by an impedance of a working electrode. So as a capacitance current is the main mechanism of a current transport at a high frequency for a big area electrode, it eliminates other processes on a counter electrode. So a potential in a cell will be divided between ohmic resistance of a cell solution and an impedance of a working electrode. After compensation of a potential loss in a cell, what is described above, the applied potential to the potentiostat will be on an interface of a working electrode. As a result, switching of the control amplifier of the potentiostat to the unity gain mode at a high frequency is defensible.

Taking into account that at a high-frequency signal propagation is determined by an interface impedance of a working electrode in a cell it is possible to realize a voltage repetition mode in potentiostat at a high frequency. It means the control amplifier has to work in normal condition with feedback from the voltage follower and in unity gain regime at a high frequency. Parameters of the filter loop (R3C1R4) between the control amplifier and the voltage follower together with parameters of R5C2 chain in a feedback loop of AD1 is selected to obtain a monotonic AC amplitude transmission characteristic. Thus the ultrafast potentiostat can work in a normal mode at a low frequency and is switched to a follower mode at a high frequency.

Correspondingly, it forms the new demand to a potentiostat utilization, ratio of a counter electrode an area to a working electrode an area must be large. This is simple to do in a cell with a micro- or a nanoelectrode as a working electrode. Rising of a signal sweep rate leads increasing of the non-Faradaic part in an electrochemical signal also. A reduction of working electrode dimensions supports a decrease of a double layer capacitance. A cell with a micro- and a nanoelectrode utilization shows a good ratio of a signal to noise response that is attractive for fast potentiostat applications [1,21].

Technical realization

A selection of electronic components is decisive for a potentiostat operation so we analyzed requirements for active elements (operational amplifiers) in this scheme (fig.1).

For the control stage, AD1, operational amplifier LM7171, National Semiconductors, was selected. LM7171 is constructed on technology-based National's advanced VIP ™ III (Vertically integrated PNP) complementary bipolar process. This OA has a very high signal slew rate at 4100 V/s, a bandwidth of a unity gain at 200 MHz, an output current up to 100 mA and supports a work with a supply voltage ±15V. This voltage determines an accessible voltage range for a polarization of a counter electrode it is little bit smaller than a supply voltage for this OA. So a supporting of a big supply voltage for this OA is welcomed. According to these parameters this OA can control a 50 Ω load. Signals to this OA come from 3 sources: i) a voltage source of a low frequency, optionally is used to control a start potential closely to equilibrium value; ii) a reference electrode feedback loop, namely a signal from AD2 through the filter; and iii) a buffer on LM7171 for a master generator of a fast signal. In a classical scheme the adder AD1 plays a potentiostat function with a limited unity gain by a slow rate signal from a reference electrode feedback loop (from AD2). In a stage of AD1 OA the feedback loop R5C2 is used for a gain limiting to unity at high frequency. Input signals are added in a connection point of resistors R1, R2, and R3. So R5, R1, R2, and (R3+R4) should be equal to obtain a correct amplification factor for each channel of signal sources.

The voltage follower, AD2 OA, is used as a current booster for a signal from a reference electrode. It is built on OA OPA627 (Texas Instrument Inc.). It contains precision high-speed field effect transistors and has the input bias current at 5 pA, the small offset potential at 100 μV with the bandwidth up to 33 MHz (the slew rate is 55 V/μs), the unity-gain stability. It is a good compromise between current sensitivity and response time in a feedback channel of a reference electrode. It also supports a supply voltage range ± 15V that is needed to ensure repeating of a reference voltage in an all polarization voltage range of a potentiostat.

The current-to-voltage converter, AD3 OA, is based on a wideband (a unity gain bandwidth is 325 MHz) FET OA THS4631, Texas Instrument, Inc. with a big slew rate (1000 V/us) and a supply voltage range above ± 15V. Although an input pins is virtually grounded in a current-to-voltage circuit, a big output voltage range and a tolerance to a high potential on inputs is result of a supporting of a wide supply voltage range. The disadvantage is the input bias current at 100 pA which is acceptable for a measurement of a current flowed through the cell from 100 nA with an accuracy of 0.1%.

For the buffers, AD4, AD5, OA OPA633, Texas Instrument, Inc. was selected. It provides the voltage slew rate at 2500 V/μs and unity gain bandwidth at 280 MHz. A high output current 100 mA is an adequate current level for a further signal transformation in the subtractor AD6 built on an amplifier LM7171, National Semiconductors.

The buffer OPA633 is characterized by a small propagation delay of a signal at 1 ns. The signal delay by subtractor OA is 5 ns. The combination of signal delays in buffers and in the current-to-voltage converter amplifier (delay 5 ns), the total time delay in the current measurement unit does not exceed 11 ns. This is constant that can be measured precisely and be corrected in experimental data as the delay between an excitation signal and a response signal in the potentiostat.

The terminators 50 or 75 Ω, coaxial cables, and sufficient connectors are used especially for a high-frequency signal transition. The high sweep rate signal incomes in the potentiostat scheme by the follower, AD7, assembled on LM7171. It adjusts impedances of a signal source generator and the potentiostat operation amplifier,

AD1. It also scales a signal two times for an amplitude restoration.

The passive components choice is important in the scheme because their parasitic characteristics insufficiently influence at low frequencies and dramatically originates at high frequencies. Chip-resistors using in the circuit minimizes parasitic capacitance and inductance. It is essential for high-frequency signal propagation. Blocking tantalum chip-capacitors are used in pairs with ceramic chip-capacitors on a power line of operational amplifiers.

One important aspect of UFP utilization is the connection to combine the signal generator, the measurement system (the oscilloscope) and the cell. The delay about 1ns is at each 30 cm of wire for electrical signals transfer. For fast sweep mode, it should be accounted [5-8]. Terminated lines, coaxial cables, and BNC connectors are utilized. In our UFP, the delay can be calculated accordingly to cables used for the connection, and it is compensated by synchronization of the generator and the oscilloscope. The cell connection to UFP is sophisticated. Utilization of a terminated line is impossible, so a wire length minimization is important. We use miniature connectors and several centimeters length wires for the cell connection. The circuit board of ultrafast potentiostat is shown in Fig.2.

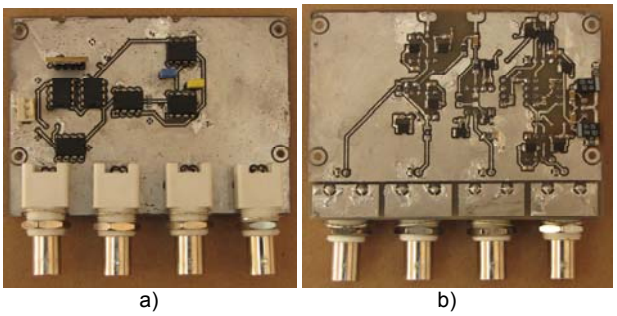

a) b)

Fig.2. Photo of ultrafast potentiostat: a) top, b) bottom view

Ultrafast potentiostat circuit simulation

The analysis of potentiostat features includes three parts: determination of AC characteristics for each unit of the potentiostat separately (the control part with the voltage follower and the current-to-voltage converter unit), and simulation of a whole potentiostat with a connected “dummy” cell. The PSpice standard description of circuit components in Multisim 11.0 software of National Instrument, Inc. was utilized. Components values effects on AC characteristics were investigated also. The response characteristic monotony was selected as the optimum. It is important to prevent oscillations in the potentiostat and to save the operation principles proposed above.

First order filters were utilized in feedback loops of the potentiostat. They were needed for a monotonic response function of the circuit. The simulation showed that smaller and bigger value of capacitance for the RCR-filter branch supports the appearance of local maximum or minimum and the optimal value only saves an AC characteristic with small distortion and monotonic in the working frequency range. The simulation with the variation of the capacitor in the control amplifier feedback loop and in the RCR filter helps to proof the capacitors selection. So parameters of both capacitors and utilized resistors should be clarified according to a selected working bandwidth limit of the potentiostat. In our case, they have values of 10 nF for the AD1 feedback loop and 5.6 nF for the filter, C2, and C1. Resistors R1, R2, R5 are 510 Ω and R3, R4 are 250 Ω and 260 Ω correspondingly. On a resistor that simulates an electrochemical cell a potential distortion is not more 0.1% till 14 MHz, a frequency gain limitation begins after 110MHz (Fig. 3).

The AC analysis of the current-to-voltage converter shows a linear magnitude AC characteristic with a fall in a high-frequency region (Fig 4.).

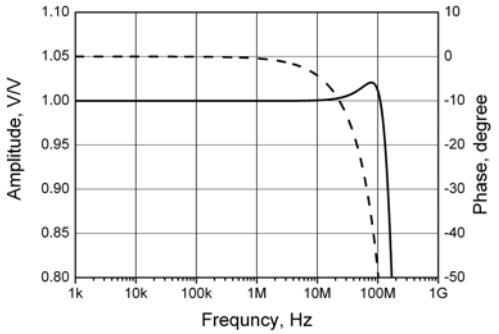

Fig.3. AC transfer characteristic for potentiostat unit (solid line – amplitude, dash line – phase characteristics)

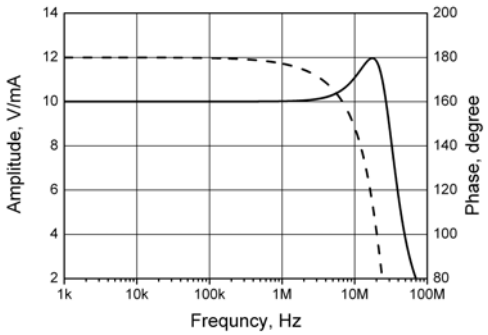

Fig.4. AC transfer characteristic for current-to-voltage converter (solid line – amplitude, dash line – phase characteristics)

A principal element in this chain of amplifiers stages is the first amplifier it’s a current-to-voltage converter. Its feedback loop determines a bandwidth of the potentiostat. Above we discussed the current detection limit and the bandwidth for potentiostat. Practical interest for selected amplifier usage is a simulation of its operation with a feedback resistor in a range of 1…100 kΩ. The small capacitor is needed in negative feedback for stability of the current-to-voltage converter amplifier. It frequently is selected experimentally in a real printed board.

Simulation results (Fig. 3-4) show the bandwidth is greater 20 MHz when components values are equal 10 kΩ for the resistor and 2 pF for the capacitor in the feedback loop. It is enough for a realization of a 1MV/s linear sweep rate. At this case a current detection level is equal to an input bias current value 100 pA, so a measurement precision for 1 uA current registration is 0.01%.

The whole potentiostat scheme operation was analyzed with the connected “dummy” cell that represents the behavior of an electrochemical cell. It includes the interface solution impedance model for three electrodes. To reduce the model the impedances were simulated by the parallel combination of the resistor and the capacitor. The linearity of characteristics is until the common capacitive load reaches to 2000pF (Fig.5). This value is too large for a microelectrode, so on the potentiostat can work with a variety of cells, solutions, and electrodes. The ohmic voltage drop compensation was verified by resistances introduction to a “dummy” cell model between the reference electrode and the working electrode to simulate the solution impedance. The corresponding resistor adding to the resistive divider in the positive feedback loop of the current-

to-voltage converter compensates the loss of voltage in the cell in the bandwidth range.

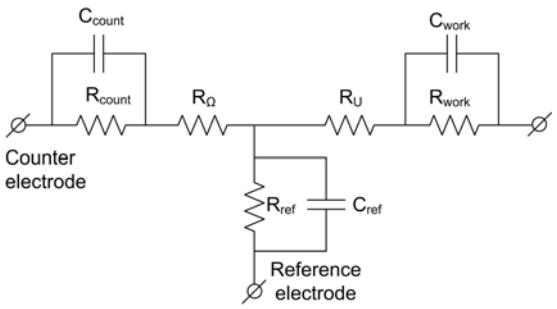

Fig. 5. "Dummy" cell for a testing (for AC characteristics measurements: C_{count} – a capacitance of a double layer for a counter electrode at 0.1 uF, R_{count} – an equivalent resistance for an electron transfer through a counter electrode-solution interface at 1 kΩ, C_{work} – a capacitance of a double layer for a working electrode, R_{work} – an equivalent resistance for an electron transfer through a working electrode-solution interface – 10 kΩ, C_{ref} –a capacitance of a double layer for a reference electrode at 10 pF, R_{ref} – an equivalent resistance for an electron transfer through a reference electrode-solution interface – 5 kΩ, a resistance of a solution between a counter electrode and a reference electrode RΩ and a resistance of a solution between a reference electrode and a working electrode R_U were 0Ω, for stability determination: Cwork – was varied in range 2…2000 pF, $R_{\Omega} + R_U$ – in range 0…1 kΩ).

Electrochemical experiment

To test of the developed potentiostat the traditional used one-electron transfer redox couple $Fe(CN)_6^{3-/4-}$ was chosen as a reversible system. In tests, we used an aqueous solution of 0.1 M $K_4[Fe(CN)_6]$ and 0.1 M $K_3[Fe(CN)_6]$ with 1M KCl supporting electrolyte. Doubly-distilled water and chemicals ACS grade of Sigma-Aldrich were utilized for solution preparation. An electrochemical cell is a cylindrical glass of 10 ml total volume filled with 5 ml the solution. The cell electrode system was mounted through holes in a polytetrafluorethylene cap. A counter electrode was a cylindrical Pt-foil with area 400 mm^2 a reference electrode was a miniature Ag/AgCl electrode. A working electrode is a gold microelectrode with a radius of 21 μm.

The excitation signal was produced by an arbitrary form generator DG3121A by Rigol, Co., connected to UFP, a data registration (an applied potential to a potentiostat, a current response signal from a potentiostat) was by a digital oscilloscope DS1204B by Rigol, Co. A powering of UFP was by a programmable power supply DP1308A by Rigol, Co. The cell, the solution, and the electrode system are the same in all experiments.

In Fig. 6 an electrochemical response for the test solution is shown. An increase of a polarization sweep rate increases a response magnitude as for current peaks as for a capacitive current it is observed here. A shift of peaks for oxidation and reduction processes is. At a higher sweep rate, a capacitive current dominates over Faradaic one, so the peak's resolution is difficult in an aqueous solution.

A hardware compensation of ohmic voltage drop is essential in electrochemical analyses as it saves sweep rate constant during a measurement and eliminates a potential loose in a cell. The voltage drop compensation is important for microelectrodes at high sweep rates as well as for macroelectrodes at low sweep rates. A feature of an ohmic drop compensation for our potentiostat was examined with an electrochemical cell described above. A result of 75 Ω ohms compensation is shown in fig.7.

Introduction of the ohmic drop compensation shifts peaks to equilibrium potential. The compensation increases a capacitive current, and results are observed at points of a potential reverse. At this moment a significant current change is because the potentiostat virtually connected to a clear capacitor that is a double layer on a working electrode. At a high sweep rate, a full ohmic compensation brings instability in the potentiostat as an oscillations appearance on an electrochemical response. Because a capacitive current is proportional to a potential sweep rate and stability of an amplifier depended by the proximity of a signal frequency to a unity gain frequency, so a chance of oscillations appearance and their magnitude also increases with a sweep rate, that point by authors in [7,8].

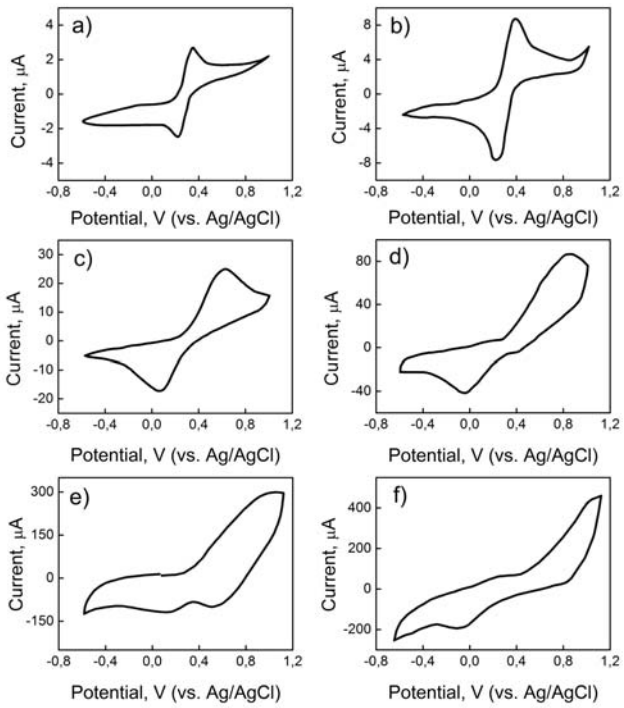

Fig. 6. CV-diagrams recorded for 0.1 M $[Fe(CN)_6]^{4-/3-}$ + 1 M KCl an aqueous solution at a sweep rate: a) 3.2 V/s; b) 32 V/s c) 320 V/s; d) 3200 V/s; e) 32 000 V/s; f) 320 000 V/s.

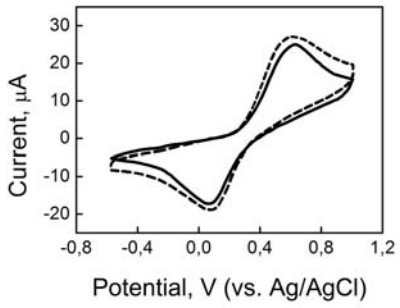

Fig 7. The effect of the ohmic voltage drop compensation on the output potentiostat signal. The potential sweep rate is 320 V/s.

Conclusion

In this work, the problem of ultrafast electrochemical potentiostat design was investigated. The analysis of traditional potentiostat electronic schemes had shown problems in measurements with a high rate for commercial instrumentation. Working principles of the fast potentiostat and the design are formulated and discussed: i) do not use interstage feedback loops, ii) minimize the number of active components, iii) the ohmic drop compensation is necessary to implement in the current-to-voltage converter stage. According to described principals, the technical realization of ultrafast potentiostat was proposed. The simulation of its electrical scheme showed a possibility for a realization of measurements in a wide frequency bandwidth that is

enough for high sweep rate electrode polarization up to 1 MV/s. Stability of the potentiostat operation with a wide range of parameters of a dummy cell indicated a good opportunity to work with different electrochemical cells, electrodes, and solutions.

Examination of UFP was done with electrochemical system 0.1 M $K_3[Fe(CN)_6]$, 0.1 M $K_4[Fe(CN)_6]$ and 1M KCl in the three electrodes electrochemical cell with a gold working microelectrode. The results confirmed ability for a work of the constructed potentiostat in a fast mode with an online compensation of an ohmic voltage drop in the cell.

Analyzing of the potentiostat circuit shows that sensitivity and time response for a potentiostat is a compromise due to a level of noises and a bandwidth of an amplifier in a current-to-voltage converter stage in a potentiostat. Selection of a current detection level for a circuit binds a possible sensitivity and maximum signal bandwidth for a potentiostat, and it is bonded directly with properties of an amplifier in the current-to-voltage converter.

The ultrafast electrochemistry advantages realized in the proposed instrumentation open a new analytical possibility that is important in many fields of electrochemistry, as for example, investigation of new nanomaterials, studies of inner stage mechanisms of quick processes like catalytic reactions. Combination of a developed potentiostat with new materials for an electrode system, a realization of extremely small working electrodes as a nanodes is a very attractive aim for the next stage of researchers.

***Authors**: Dmytro V. Snizhko, Associate Prof., PhD, Department of Biomedical Engineering, Kharkiv National University of Radio Electronics, Nauky ave., 14, Kharkiv, Ukraine 61066, E-mail: dmytro.snizhko@nure.ua; Anatolii V. Kukoba, Associate Prof., PhD, Department of Biomedical Engineering, Kharkiv National University of Radio Electronics, Nauky ave., 14, Kharkiv, Ukraine 61066, E-mail: anatolii.kukoba@nure.ua;*

REFERENCES

[1] Robert J. Forster, 2.5 Miroelectrodes – Retrospect and Prospect, in: Encyclopedia of Electrochemistry, Vol.3, Instrumentation and Electroanalytical Chemistry, A.J. Bard, M. Stratmann, P. R. Unwin (Eds.), Wiley, New York, 2003, 170.

[2] C.P. Andrieux, D. Garreau, P. Hapiot, J. Pinson, J.M. Savéant, Fast sweep cyclic voltammetry at ultra-microelectrodes. Evaluation of the method for fast electron-transfer kinetic measurements, J. of Electroanal. Chem., 243 (1988) 321-335.

[3] C.P. Andrieux, D. Garreau, P. Hapiot, J.M. Savéant, Ultramicroelectrodes: cyclic voltammetry above one million V s^{-1}, J. of Electroanal. Chem. and Interfacial Electrochem. 248(1988) 447-450.

[4] J.O. Howell , R.M. Wightman, Ultrafast voltammetry of anthracene and 9,10-diphenylanthracene . J. of Phys. Chem. 88 (1984) 3915-3918.

[5] C. Amatore, C. Lefrou, F. Pflüger, On-line compensation of ohmic drop in submicrosecond time resolved cyclic voltammetry at ultramicroelectrodes, J. of Electroanal. Chem. 270 (1989) 43-59.

[6] C. Amatore , C. Lefrou, New concept for a potentiostat for on-line ohmic drop compensation in cyclic voltammetry above 300 kV s-1. J. of Electroanal. Chem. 324 (1992) 33-58.

[7] C. Amatore, E. Maisonhaute, G. Simonneau, Ultrafast cyclic voltammetry: performing in the few megavolts per second range without ohmic drop, Electrochem. Commun., 2 (2000), 81-84.

[8] C. Amatore, E. Maisonhaute, G. Simonneau, Ohmic drop compensation in cyclic voltammetry at scan rates in the megavolt per second range: access to nanometric diffusion layers via transient electrochemistry, J. of Electroanal. Chem. 486 (2000) 141-155.

[9] P. Fortgang, C. Amatore, E. Maisonhaute, B. Schollhorn, Microchip for ultrafast voltammetry, Electrochem. Commun. 12 (2010) 897-900.

[10] Z. Guo, X. Lin , Ultrafast cyclic voltammetry at scan rates of up to 3 MV s^{-1} through a single-opamp circuit with positive feedback compensation of ohmic drop, J. of Electroanal. Chem., 568 (2004) 45-53.

[11] Z. Y. Guo, X. Q. Lin, Ultrafast cyclic voltammetry with asymmetrical potential scan, Chin. Chem. Lett., 19(2008) 85-88.

[12] D.O. Wipf, R.M. Wightman, Submicrosecond measurements with cyclic voltammetry, Anal. Chem., 60 (1988) 2460-2464.

[13] R.M. Wightman, D.O. Wipf, High-speed cyclic voltammetry. Accounts of Chem. Res., 23 (1990) 64-70.

[14] C. Amatore, G. Farsang, E. Maisonhaute, P. Simon, Voltammetric investigation of the anodic dimerization of p-halogenoanilines in DMF: Reactivity of their electrogenerated cation radicals, J. Electroanal. Chem., 462 (1999) 55-62.

[15] C. Amatore, Y. Bouret, E. Maisonhaute, J. I. Goldsmith, H. D. Abruña, Ultrafast voltammetry of adsorbed redox active dendrimers with nanometric resolution: An electrochemical microtome, ChemPhysChem, 2 (2001) 130-134.

[16] C. Amatore, Y. Bouret, E. Maisonhaute, J.I. Goldsmith, H.D. Abruña, Precise adjustment of nanometric-scale diffusion layers within a redox dendrimer molecule by ultrafast cyclic voltammetry: An electrochemical nanometric microtome, Chemistry - A European Journal, 10 (2001) 2206-2226.

[17] C. Amatore, Y. Bouret, E. Maisonhaute, H. D. Abruña, J.I. Goldsmith, Electrochemistry within molecules using ultrafast cyclic voltammetry, Comptes Rendus Chimie, 6 (2003), 99-115.

[18] N. V. Rees, O. V. Klymenko, E. Maisonhaute, B. A. Coles, R.G. Compton, The application of fast scan cyclic voltammetry to the high speed channel electrode, J. of Electroanal. Chem. 542 (2003) 23-32.

[19] Z. Guo, X. Lin, Kinetic studies of dioxygen and superoxide ion in acetonitrile at gold electrodes using ultrafast cyclic voltammetry, J. of Electroanal. Chem., 576 (2005) 95-103.

[20] C.A. Amatore , A. Jutand, F. Pflüger, Nanosecond time resolved cyclic voltammetry: Direct observation of electrogenerated intermediates with bimolecular diffusion controlled decay using scan rates in the megavolt per second range, J. of Electroanal. Chem. and Interfacial Electrochem., 218 (1987) 361-365.

[21] C. Amatore, Chap. 4. Electrochemistry at Microelectrodes, in: Physical Electrochemistry: Principles, Methods and Applications, I. Rubinstein (Ed.), Marcel Dekker, New York, 1995, 131–208.

[22] Amatore, C., Maisonhaute, E., Nierengarten, J.-F., Schöllhorn, B. Direct Monitoring of Ultrafast Redox Commutation at the Nanosecond and Nanometer Scales by Ultrafast Voltammetry: From Molecular Wires to Cation Releasing Systems, Israel J. of Chem., 48 (2008) 203-214.

[23] Zhou, X.-S., Liu, L., Fortgang, P., Lefevre, A.-S., Serra-Muns, A., Raouafi, N., Amatore, C., Mao, B.-W., Maisonhaute, E., Schöllhorn, B. Do molecular conductances correlate with electrochemical rate constants? Experimental insights, JACS, 133 (2011), 7509-7516.

[24] C. Amatore, E. Maisonhaute, B. Schçllhorn, J. Wadhawan, Ultrafast voltammetry for probing interfacial electron transfer in molecular wires, ChemPhysChem. 8 (2007) 1321–1329.

[25] A. J. Bard & L.R. Faulkner Chap. 15 Electrochemical instrumentation, in: A. J. Bard & L.R. Faulkner, Electrochemical Methods: Fundamentals and Applications, John Wiley & Sons, Inc., New York, 2000, 632-658.

[26] D. Wipf, Chap. 1.2 Analog and Digital Instrumentation, in: Vol.3, Instrumentation and Electroanalytical Chemistry, A.J. Bard, M. Stratmann, P. R. Unwin (Eds.), Wiley, New York, 2003, p. 24-50.

[27] J. Dostal, Operational Amplifier, Sec. Eds., Butterworth-Heinemann, 1993.